High-pressure phases of crystalline tellurium: A combined Raman and *ab initio* study

C. Marini,[1,2] D. Chermisi,[1] M. Lavagnini,[3] D. Di Castro,[4] C. Petrillo,[5] L. Degiorgi,[3] S. Scandolo,[6] and P. Postorino[1]

[1]*Dipartimento Fisica, Universitá di Roma "Sapienza", P.le A. Moro 2, I-00185 Roma, Italy, and CNR-IOM*

[2]*European Synchrotron Radiation Facility, 6 Rue Jules Horowitz, BP220, 38043 Grenoble Cedex, France*

[3]*Laboratorium für Festkörperphysik, ETH-Zürich, CH-8093 Zürich, Switzerland*

[4]*CNR-SPIN and Dipartimento di Ingegneria Informatica Sistemi e Produzione, Università di Roma "Tor Vergata", Via del Politecnico 1, I-00133 Roma, Italy*

[5]*Dipartimento di Fisica Universitá di Perugia and CNR-IOM, Unitá di Perugia Via Alessandro Pascoli, I-06123 Perugia, Italy*

[6]*"Democritos" CNR-INFM National Simulation Centre, Trieste, Italy and The Abdus Salam International Centre for Theoretical Physics, Trieste, Italy*

(Received 19 June 2012; published 9 August 2012)

A room temperature study of the high-pressure phases of crystalline Te was carried out by combining Raman spectroscopy and density functional theory (DFT)-based calculations. The pressure dependence of the experimental phonon spectrum reveals the occurrence of phase transitions, confirming the high-pressure scenario recently proposed by Hejny and McMahon. The effects of the incommensurate lattice modulation on the vibrational properties of Te are discussed. DFT-based calculations are consistent with the present and previous experimental data and show that the metallization process at 4 GPa is due to charge-bridges between atoms belonging to adjacent chains. A first-principles study of the stability of the 4 GPa phase is here reported and discussed against the insurgence of lattice modulation.

DOI: 10.1103/PhysRevB.86.064103 PACS number(s): 62.50.−p, 31.15.E−, 63.20.−e, 71.30.+h

I. INTRODUCTION

Recent investigations of the pressure-induced structural evolution in several elements (mostly Chalcogens and Halogens, such as S, Se, Te, I, and Br) have provided evidence for the onset of a high-pressure (HP) incommensurately modulated (IM) lattice arrangement. These findings suggest the idea that the development of aperiodic structures is a common phenomenon in elemental systems under pressure.[1–7] Moreover, in a variety of those, e.g., I, Br, P, S, Se, and Te, the overall picture is even more intriguing, since applied pressure induces a metallization transition preceding the onset of the IM phase, which suggests a connection of the IM phase with an electronic instability.[7] In this context, Te is a prototype system well suited for an experimental[6–8] and theoretical[9,10] investigation of the crystalline and electronic structure stability under pressure. It is well known that, at ambient conditions and for pressures up to 4 GPa, Te is a semiconductor and its crystal structure is trigonal with spiral atom chains along the c axis (Te-I). The three atoms in the unit cell are linked via covalent-like bonds to the nearest neighbors along the chain, and via Van der Waals interactions to the second neighbors lying along adjacent chains.[11] The very HP regime (i.e., above 27 or 29 GPa, according to Ref. 12 or 6, respectively) is also well established, namely Te is a metal with a highly symmetric bcc structure (Te-IV). A metallization transition is also known to occur at 4 GPa.[8]

Despite these data, the structural behavior in the intermediate pressure range remained controversial for a long time. Starting from the early '80s, the generally accepted phase diagram accounts for four phases: a puckered layer monoclinic structure for $P > 4$ GPa, which transforms into orthorhombic at 6.8 GPa and finally a β-Po-type between 11 GPa and the Te-IV pressure threshold.[11–13] Recent x-ray diffraction (XRD) measurements[6,14] have drawn a rather different HP scenario, claiming a structural transition to triclinic (Te-II) at 4.0 GPa, followed by the onset of an IM monoclinic phase (Te-III) at 4.5 GPa, which is finally transformed into the bcc Te-IV phase above 29 GPa. It is worth noticing that since Te-I is observed up to 4.5 GPa and Te-II up to 8 GPa, we have large regions of coexisting phases, and the above reported phase boundaries are intended as the pressure threshold at which the higher pressure phase first appears on compressing the lattice. The comparison between the two proposed phase diagram schemes is summarized in Table I.

Vibrational spectroscopy can represent an alternative tool to XRD to investigate structural phase transitions as well as to understand the bonding characteristics. It is particularly effective when coupled to a theoretical analysis. In the present paper, a combination of experiments and *ab initio* calculations is applied to analyze the HP behavior of solid Te aiming at gaining a deeper insight into the microscopic modifications induced by pressure. Actually, HP Raman spectra have been collected in Te over the 0- to 15-GPa pressure range and compared with DFT-based calculations. Combining experimental and theoretical results, the role of first- and second-neighbor chains is addressed to understand the effects of dynamics on both electronic and structural transitions.

II. EXPERIMENT

A high-purity Te sample (99.99% by Aldrich) was used without further treatment. HP Raman measurements were carried out using a diamond anvil cell coupled to a microRaman spectrometer (Horiba Jobin Yvon). The ruby fluorescence technique was employed for pressure calibration, and two series of measurements using different pressure-transmitting media (NaCl and methanol-ethanol 1:4 mixture) were carried out to verify the presence of possible spurious effects on the high-pressure Te spectra. Moreover, exploiting the high spatial

TABLE I. Comparison between phase transition schemes after Refs. 11–13 and Refs. 6 and 14, respectively. (*) 27 or 29 GPa are the low-pressure boundary at Te-IV phase according to Ref. 12 or 6. (**) The structural phase is incommensurately modulated.

Phase diagram from Refs. 11– 13		Phase diagram from Refs. 6 and 14	
Pressure (GPa)	Structure	Pressure (GPa)	Structure
0–4	Te-I (trigonal)	0–4	Te-I (trigonal)
4–7	Monoclinic	4–4.5	Te-I + Te-II (trigonal + triclinic)
7–11	Orthorhombic	4.5–8	Te-II + Te-III (triclinic + monoclinic)
11–27 (29)*	Rhombohedrical	8–29	Te-III**
>27 (29)*	Te-IV (bcc)		Te-IV (bcc)

resolution of our experimental setup, Raman spectra at each pressure value were collected from different points over the surface of the sample (about $50 \times 50\ \mu m^2$) to test the presence of pressure gradients. Further details on the experimental setup and on data analysis can be found in Ref. 15. Here we just notice that great care was taken in the optical alignment[16] to collect reliable spectra starting from 80 cm^{-1}, and that we did not find any evidence of either reactions between the media and the sample or detectable nonhydrostaticity effects. No laser-induced sample heating was observed.[17]

III. RESULTS AND DISCUSSION

Normalized and background subtracted Raman spectra of Te, collected using NaCl and methanol-ethanol are shown in Fig. 1 at selected pressure values. Measured spectra were fitted by using a standard model curve[18] given by the sum of three phonon contributions (each described by a damped harmonic oscillator) and an electronic background.[15] A linear baseline was also included in the fitting curve. According to the standard group theory (GT), the irreducible representation of the optical modes of Te-I is $A_1 + A_2 + 2E$. The Raman active modes are: the A_1 mode (breathing in the *ab* plane) and the two doubly degenerate E modes ($E(1)$ *a*- and *b*-axis rotation, $E(2)$ asymmetric stretching mainly along *c*axis). The latter two modes are also Infrared active since the crystal lacks a center of inversion. In Fig. 1(b), the best-fit curve and the Te-I phonon assignment are shown as an example for the spectrum at the lowest pressure value, namely 1.8 GPa. The spectra shown in Figs. 1(a) and 1(b) are background subtracted and normalized to the phonon integrated intensities.

The Raman spectrum shows a remarkable pressure dependence, albeit the three-peaks structure is basically preserved over the whole pressure range. The irreducible representation for the Te-II phase is $\Gamma = 3A_g + 3A_u$ where the three A_g modes are Raman active. We notice that the persistence of a Raman signal well above 11 GPa contradicts the first proposed phase transition scheme,[11–13] since no Raman-active modes are expected for the β-Po-type phase. On the other hand, an unmodulated monoclinic phase (i.e., an unmodulated Te-III structure) does not show Raman-active modes, as well. The observation of a Raman signal above 11 GPa is thus consistent only with the newly proposed transition scheme, where the

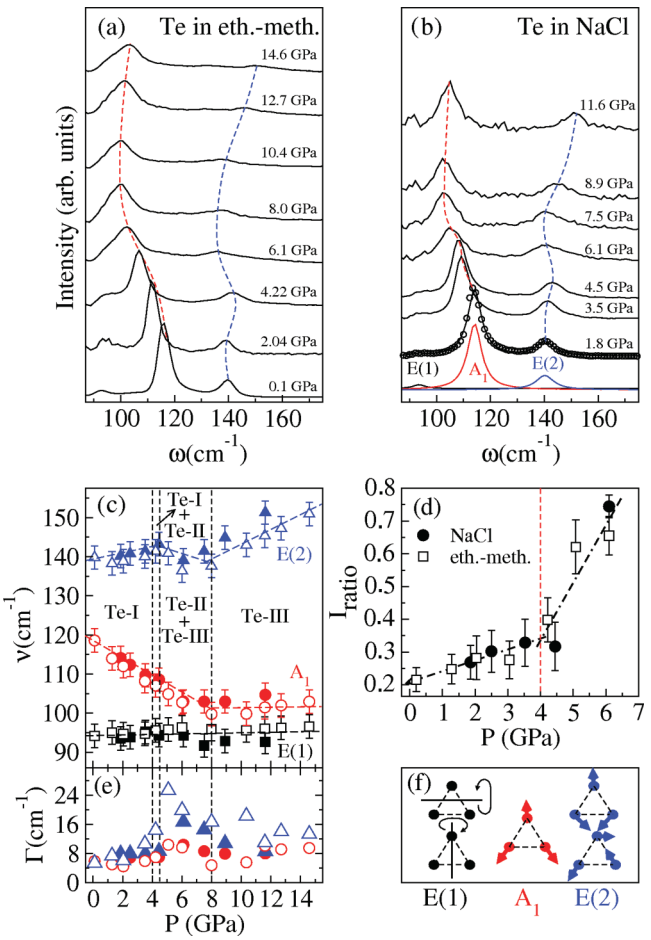

FIG. 1. (Color online) Te Raman spectra at RT and selected P, in ethanol-methanol (a) and NaCl (b). Best-fit curve and phonon contributions for the $P = 1.8$ GPa spectrum are also shown in (b). P dependence of phonon frequencies (c) and linewidths (e). Vertical lines in (c) and (e) mark the phase transitions pressures according to Ref. 14. The intensity $I_{ratio} = I[E(2)]/(I[E(1)] + I[A_1])$ (see text) vs. pressure in (d). Open (close) symbols in (c), (d), and (e) refer to measurements using ethanol-methanol mixture (NaCl). Color code and atomic displacements for the Raman active modes in Te-I (f).

Te-III structure appears to be of IM nature.[6] Indeed, optical scattering processes are, in this case, allowed not only from phonons at Γ but, according to the phonon dispersion treated in sinusoidal approximation, also at $k = \pm q_i$ (with q_i the modulation wave vector). Using the superspace GT (equations and formalism are from Ref. 19), the calculated character of the representation is $\chi(E,2_y,m_y,I) = (6,2,0,0)$, where $E, 2_y, m_y$, and I denote the point group operations of the three-dimensional space-group elements. This representation is reducible into $\Gamma = 2A_g + 1B_g + 2A_u + 1B_u$, where three Raman active modes (two A_g modes and the B_g mode) are expected. The presence of the three peaks in the high-pressure spectra of Fig. 1 is clear experimental evidence in support of the recently proposed transition scheme, which can be seen as a marker of the onset of an IM phase.[6,14] We want to stress that, for the sake of simplicity, we improperly use the same labels $[E(1), A_1, E(2)]$ for the three Raman peaks observed over the whole explored pressure range, although the symmetry is A_g for the three active mode of Te-II and $2A_g + 1B_g$ for those of Te-III incommensurately modulated phase.

Looking at Fig. 1(c), where the values of the best-fit parameters for frequency and linewidth are shown, three different pressure regions can be identified by the slope change of the observed pressure dependencies. The boundaries between these regions actually correspond to the pressure thresholds of the new transition scheme.[6,14] Over the 0- to 4-GPa pressure range, the phonon frequency of the A_1 mode (chain breathing) shows a linear softening ($\sim$10 cm^{-1}), whereas the frequencies of the two E modes show a weak increase. Over the same pressure range, a contraction of the b lattice parameter is observed, while c keeps almost constant,[11] which suggests a progressive weakening of intrachain bonds in favor of interchain atomic interactions. The slope discontinuity of the pressure dependence of the $E(2)$ mode, whose frequency starts to decrease at 4 GPa, marks the appearance of a new crystal phase although, within 4–7 GPa, the frequency of the A_1 phonon is still decreasing and that of the $E(1)$ mode remains almost constant. The narrow pressure range in which Te-I and Te-II coexist (4–4.5 GPa) makes it impossible to determine whether the discontinuity can be ascribed to the Te-I and Te-II transition or to the onset of the Te-III phase. According to Refs. 6 and 14, where the Te-II and Te-III coexistence is reported over the 4.5- to 8-GPa pressure range, the observed softening of the $E(2)$ mode can be ascribed to the structural instability of the Te-II phase that is progressively converted into the rather similar Te-III phase. We observe that larger values of the phonon linewidths [Fig. 1(e)] are found within the coexistence region (4.5–8 GPa), with respect to the other pressure range, as a consequence of the lattice disorder. On further increasing the pressure above 8 GPa, all the phonon modes show a rather regular frequency hardening, indicating that a single, stable phase (Te-III) has finally established.

As previously mentioned, the incommensurate modulation of the Te-III phase allows us to detect a Raman signal from phonons not only at Γ but also at a momentum transfer equal to the modulation vector (i.e., $k = \pm q_i$).[19] Indeed, we note that the Raman frequency of the $E(2)$ mode at 8.9 GPa [Te-III phase; see Fig. 1(c)], is the same, within the experimental uncertainties, as the frequency of the longitudinal mode at $k = \pm q_i$ observed in a recent inelastic x-ray scattering experiment.[7] This finding provides further evidence of the onset of an IM phase at HP.

The weakening of intrachain bonds can be ascribed to the onset of a pressure-induced charge transfer process, as also suggested by the remarkable reduction of the intensity (peak integrated area) of the A_1 mode, $I[A_1]$.[20] This effect is shown in Fig. 1(d), where the pressure dependence of the intensity ratio $I_{\text{ratio}} = I[E(2)]/(I[A_1] + I[E(1)])$ is shown. Neglecting the little contribution to I_{ratio} due to the small intensity (area) of the $E(1)$ mode, the increase of I_{ratio} corresponds to the intensity decrease of the A_1 peak before the metallization pressure.[20] Two different regimes, below and above the metallization pressure (4 GPa), can be clearly identified.

To gain further insight into the microscopic charge-transfer process, pseudopotential DFT-based calculations have been carried out using the Quantum-Espresso code.[21] Preliminary tests showed that the energy and the forces on atoms are well converging in the case of Te-I using a plane waves cutoff of 82 Ryd and a $7 \times 7 \times 7$ Monkhorst-Pack of $343 = 7^3$ k points. We also accounted for systematic error, known as Pulay stress, in the determination of the external pressure. Further details and specific data about DFT calculations can be found in Ref. 22. A full structural relaxation under the influence of Hellmann-Feynman forces and stresses was carried out for Te-I at 0, 2.5, and 5 GPa using the variable cell shape method.[23] At each pressure, the electron density of states and bands, as well as the frequencies and the intensities of normal vibrational modes, were obtained by the perturbation approach of DFT.[24] We found closure of the energy gap at 5 GPa and an overall good agreement between the calculated data and the experimental structural data at HP.[11] The intrachain bond length was slightly overestimated because of the typical error of the generalized gradient approximations in the determination of the cohesive force in strongly anisotropic systems. This results in an underestimate of the calculated phonon frequencies (by less than 10%), which, however, together with the intensity ratio I_{ratio} defined above, shows the same pressure dependence as the experimental data. Moreover, calculations support the evidence for a progressive reduction of the angle between the $E(2)$ mode eigenvectors and the c axis on applying pressure (from 12° at $P = 0$ to 2.5° at $P = 5$ GPa). The good agreement of the results of DFT-based calculations with the present and the previous experimental data made us confident also about the other possible outputs of the code. In particular, our calculations provided also the maps of the valence electron ($5s^2 5p^4$) densities at ambient pressure and 5 GPa, shown in Fig. 2. The onset of a bridge of charge density linking the atoms inside the chain and the first neighbor atom in the adjacent chain is pretty clear at $P = 5$ GPa. The metallization transition is therefore the result of the simultaneous lattice symmetrization and charge-transfer processes from intrachain to interchain regions, which enables the mobility of the valence electrons. This is a pressure-induced (i.e., density induced) mechanism that closely resembles the intra- to intermolecular charge transfer processes observed in the metallization transition of molecular elemental systems (e.g., iodine; see Refs. 20 and 25).

We also exploited the DFT approach to investigate the structural Te-I/Te-II transition. In Te-I, most of the crystallographic constants are fixed by the hexagonal geometry. Nevertheless,

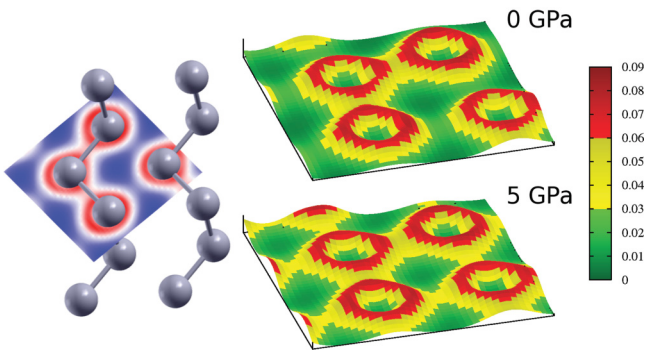

FIG. 2. (Color online) Valence electron density at 0 and 5 GPa in the Te-I phase over the plane containing three atoms along the chain and the closest atom in the adjacent chain.

the DFT underestimates the anisotropy of the system leading to a slight overestimation of the ratio of chain radius to interchain distance. We notice that in the Te-II structure each layer is shifted alternately by a half a lattice constant along the *b* axis and it is stacked in the *c* axis direction. In the Te-II case, where all the lattice parameters and the atom positions are left free to vary during the cell relaxation, this trend is strongly emphasized. Therefore, with relaxing the structure, the experimental zig-zag puckering is entirely lost. For this reason, the dynamic properties for the Te-II relaxed cells in the pressure range between 3.5 and 7 GPa differ qualitatively from the experimental ones, even if the calculated enthalpy of the Te-I phase becomes higher than that of Te-II phase above 5.5 GPa, in agreement with the occurrence of the phase transition (see Fig. 3).

Thus, the dynamical properties were calculated optimizing the atomic positions, while keeping the lattice parameters fixed to the experimental values obtained for the Te-II phase at 4.5 GPa.[14] For the sake of comparison, the Raman frequencies have been recalculated by optimizing only the atomic positions keeping the lattice parameters constant and equal to the experimental values observed for the Te-I phase

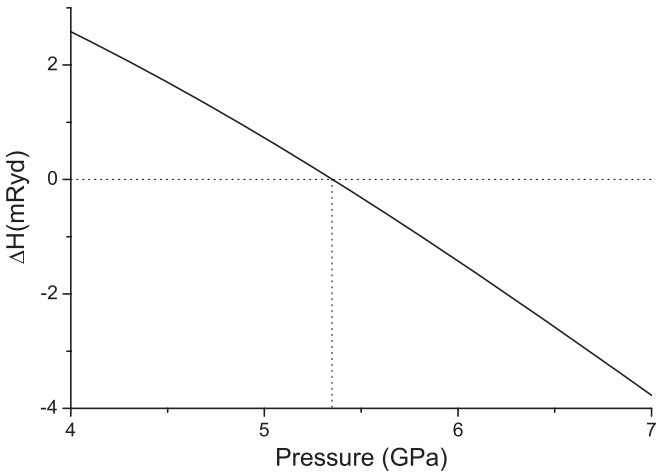

FIG. 3. The difference $\Delta H = H_{\text{Te-II}} - H_{\text{Te-I}}$ between the enthalpy values of the Te-II and Te-I cells relaxed at different pressures using the variable cell shape method. Dotted lines mark the crossover.

TABLE II. Calculated Raman phonon frequencies for Te-I and Te-II optimizing the atom positions while keeping constant the lattice parameters to the experimental values.

Te-I at 4 GPa		Te-II at 4.5 GPa	
Mode	ν (cm^{-1})	Mode	ν (cm^{-1})
E(1)	78	$A_g(1)$	38
A_1	92	$A_g(2)$	94
E(2)	122	$A_g(3)$	125

at 4.0 GPa. The results for the two phases are reported in Table II.

We observe that only the so calculated value of the low-frequency phonon shows a remarkable discontinuity at the transition, whereas for the high-frequency modes the differences between the values calculated in the two phases are within the typical DFT calculations accuracy. Thus, in agreement with the experimental data, our calculations predict a continuous evolution of the frequencies across the Te-I to Te-II transition for the high-energy modes. As to the estimate of the frequency of the low-energy mode, further discussion is required. This vibrational mode is that mostly affected by the IM phase since the direction of the incommensurate modulation is rather close to the direction along which the atom displacements occur. The underestimate of the mode frequency seems to be related to an excessive sensitivity of the DFT theory to predict the IM phase, or in other words it seems to be related to an overestimate of the width of the saddle point of the energy landscape in the direction of the modulation. This is confirmed by the fact that there is a neighborhood of points around q_i for which the transverse acoustic phonon has negative energies.[7]

IV. CONCLUSIONS

In summary, we present a high pressure study of crystalline Te, using a combined approach of experimental spectroscopic with *ab initio* calculations to address the complexity of this system. Our Raman data confirms the recently proposed HP phase scenario.[6] The analysis of the Raman spectra collected above 8 GPa, combined with recent inelastic x-ray scattering measurements,[7] suggests IM occurrence of the Te-III phase over this pressure range. Our DFT calculations well reproduce the experimental data, allowing for an accurate and systematic investigation of the microscopic modifications of both structural and electronic dynamics under lattice compression: the metallization transition is driven by an intra- to interchain charge transfer, which develops charge density bridge among adjacent chains.

ACKNOWLEDGMENT

L.D. acknowledges support by the Swiss National Foundation for the Scientific Research within the NCCR MaNEP pool.

[1]T. Kenichi, S. Kyoko, F. Hiroshi, and O. Mitsuko, Nature **423**, 971 (2003).
[2]T. Kume, T. Hiraoka, Y. Ohya, S. Sasaki, and H. Shimizu, Phys. Rev. Lett. **94**, 065506 (2005).
[3]R. J. Nelmes, D. R. Allan, M. I. McMahon, and S. A. Belmonte, Phys. Rev. Lett. **83**, 4081 (1999).
[4]H. Fujihisa, Y. Akahama, H. Kawamura, Y. Ohishi, Y. Gotoh, H. Yamawaki, M. Sakashita, S. Takeya, and K. Honda, Phys. Rev. Lett. **98**, 175501 (2007).
[5]O. Degtyareva *et al*., Nat. Mater. **4**, 152 (2005).
[6]C. Hejny and M. I. McMahon, Phys. Rev. Lett. **91**, 215502 (2003).
[7]I. Loa, M. I. McMahon, and A. Bosak, Phys. Rev. Lett. **102**, 035501 (2009).
[8]J. Bardeen, Phys. Rev. **75**, 1777 (1949).
[9]H. C. Hsueh, C. C. Lee, C. W. Wang, and J. Crain, Phys. Rev. B **61**, 3851 (2000).
[10]H. Akbarzadeh and M. R. Mohammadizadeh, Comp. Mat. Sci. **8**, 335 (1997).
[11]K. Aoki, O. Shimomura, and S. Minomura, J. Phys. Soc. Jpn. **48**, 551 (1980).
[12]G. Parthasarathy and W. B. Holzapfel, Phys. Rev. B **37**, 8499 (1988).
[13]J. C. Jamieson and D. B. McWhan, J. Chem. Phys. **43**, 1149 (1965).
[14]C. Hejny and M. I. McMahon, Phys. Rev. B **70**, 184109 (2004).
[15]P. Postorino, A. Congeduti, E. Degiorgi, J. P. Itié, and P. Munsch, Phys. Rev. B **65**, 224102 (2002).
[16]M. Lavagnini, M. Baldini, A. Sacchetti, D. Di Castro, B. Delley, R. Monnier, J.-H. Chu, N. Ru, I. R. Fisher, P. Postorino, and L. Degiorgi, Phys. Rev. B **78**, 201101 (2008).
[17]A. Paolone, A. Sacchetti, T. Corridoni, P. Postorino, R. Cantelli, G. Rousse, and C. Masquelier, Solid State Ionics **170**, 135 (2004).
[18]A. Congeduti, P. Postorino, E. Caramagno, M. Nardone, A. Kumar, and D. D. Sarma, Phys. Rev. Lett. **86**, 1251 (2001).
[19]T. Janssen, J. Phys. C **12**, 5381 (1979).
[20]A. Congeduti, P. Postorino, M. Nardone, and U. Buontempo, Phys. Rev. B **65**, 014302 (2001).
[21]QUANTUM-ESPRESSO is a community project for high-quality quantum-simulation software, based on density-functional theory, and coordinated by Paolo Giannozzi. See http://www.quantum-espresso.org and http://www.pwscf.org.
[22]D. Chermisi, Ph.D. thesis, University of Rome, "Sapienza," 2010, http://www.phys.uniroma1.it/DipWeb/dottorato/DOTT_FISICA/MENU/03DOTTORANDI/TesiFin23/Chermisi.pdf.
[23]R. M. Wentzcovitch, Phys. Rev. B **44**, 2358 (1991).
[24]S. Baroni, S. de Gironcoli, A. Dal Corso, and P. Giannozzi, Rev. Mod. Phys. **73**, 515 (2001).
[25]U. Buontempo, A. Filipponi, P. Postorino, and R. Zaccari, J. Chem. Phys. **108**, 4131 (1998).